Chapter 5

Docking Studies on Novel Analogues of 8-Chloro-Quinolones against *Staphylococcus aureus*

Lucia Pintilie and Amalia Stefaniu

Additional information is available at the end of the chapter

http://dx.doi.org/10.5772/intechopen.72995

Abstract

Molecular docking studies have been carried out for a better understanding of the drug-receptor interactions. All the synthesized compounds have been subjected to molecular docking against targets that have been chosen based on the specific mechanism of action of the quinolones used in the antibacterial activity screening. A study of the characteristics and molecular properties of the small molecule known as ligand has been realized. In the first stage of the study, the 2D and 3D structures have been generated. The most stable conformer for each structure was obtained by geometry optimization and energy minimization. A series of topological, conformational characteristics and QSAR properties, important to assess the flexibility and the ability of the studied conformer to bind to the protein receptor, were determined and analyzed. These properties were discussed in order to assess the flexibility and the binding ability of studied conformers to bind to the receptor protein. The docking studies have been carried out. The score and hydrogen bonds formed with the amino acids from group interaction atoms are used to predict the binding modes, the binding affinities and the orientation of the docked quinolones in the active site of the protein receptor.

Keywords: molecular docking, antimicrobial activity, fluoroquinolones, quinolones

1. Introduction

An important parameter in the development of a new drug is the drug's affinity to the identified target (protein/enzyme). Predicting the ligand binding to the target (protein/enzyme) by molecular simulation would allow the synthesis to be restricted to the most promising compounds [1–9]. Molecular docking can be accomplished by two interdependent steps [7–9]. The first step consists in sampling the ligand conformations in the active site of the protein receptor. The second step is to classify these conformations by a scoring function. The sampling algorithms

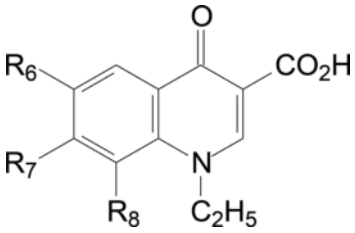

Figure 1. The structure of the quinolone compounds.

should be able to reproduce experimental binding mode. Various algorithms used for docking analysis are molecular dynamics, Monte Carlo methods, genetic algorithms, fragment-based methods, point complementary methods and distance geometry methods, systematic searches. The scoring function should classify the highest among all the generated conformations. These mathematical models are used to predict the strength of binding affinity called noncovalent interaction between two molecules after they have been docked. They have also developed scoring function to predict the strength of other types of intermolecular interactions, for example, between two proteins or between proteins and DNA or protein and drug. These configurations are evaluated using the scoring functions to distinguish experimental binding modes of all other ways explored by the search algorithm. The goal of molecular docking is to predict the ligand-receptor complex structure by computation method to identify new active molecules that bind to a biological target [10–14]. The main methods used for docking are Lock and Key/Rigid Docking and Induced Fit/Flexible Docking. In rigid docking, the internal geometry of the receptor and ligand is kept fixed and docking is performed. In flexible docking, enumeration on the rotations of one of the molecules (usually smaller one) is performed. Every rotation, the surface cell occupancy and energy are calculated; later, the most optimum pose is selected.

This chapter presents design and molecular docking studies about 8-chloro-quinolone compounds. The influence of the presence of chlorine atom in the eighth position of the quinolone ring (**Figure 1**, where R_8 = Cl) on the antimicrobial activity against *Staphylococcus aureus* has been studied. The predicted activity has been correlated with the experimental activity who has been determined by agar dilution method [15, 16].

Drugs belonging to the quinolone compound are characterized by a quicker biological activity and a larger antibacterial spectrum. They are active on both gram-positive and gram-negative bacteria, as well as on recently discovered bacteria with intercellular development (Legionella, Mycoplasma, etc.), or even on acid-resistant bacteria (*M. tuberculosis* and *M. leprae*). The area of use of quinolones has expanded from urinary infections to systemic acute and chronic infections (lung and bronchus infections, osteitis, septicemia and endocarditis, chronic infections [chronic bronchitis, purulent osteoarthritis, chronic prostatite, cystitis and chronic sinusitis]) [15, 16].

2. Materials and methods

Molecular docking studies have been performed with CLC Drug Discovery Workbench Software in order to achieve accurate predictions on optimized conformation for both the quinolone (as

ligand) and their target receptor protein to form a stable complex. Molecular docking studies have been performed on topoisomerase II DNA gyrase with 32 quinolone compounds to understand the binding affinity of all quinolones with DNA gyrase. The crystal structure of topoisomerase II was downloaded from Protein Data Bank (PDB ID: 2XCT) [17]. The quinolone compounds have been synthesized in our laboratory [16], and their structures are shown in **Figure 1** and **Table 1**.

2.1. Ligand preparation

The ligands have been prepared using SPARTAN'14 software package [18]. In this study, the DFT/B3LYP/6–31G* level of basis set has been used for the computation of molecular structure, vibrational frequencies and energies of optimized structures (**Figure 2**). In order to perform structure–activity relationship (SAR) studies, some electronic properties (**Table 2**) such as highest occupied molecular orbital (HOMO) and lowest unoccupied molecular orbital (LUMO) energy values, HOMO and LUMO orbital coefficient distribution, molecular dipole moment, polar surface area (PSA), the ovality, polarizability, the octanol water partition coefficient (logP), the number of hydrogen-bond donors (HBDs) and ad acceptors (HBAs) and acceptor sites (HBAs) and positive and negative ionizable sites are derived from CFD assignments. HBA/HBD and ±Centers, Hydrophobe Centers including aromatic centers, can be viewed in **Figure 2**, for the quinolones FPQ 28 and 6ClPQ 28 (compounds that showed good activity against MRSA [19]). The polarizability is useful to predict the interactions between nonpolar atoms or groups and other electrically charged species, such as ions and polar molecules having a strong dipole moment.

2.1.1. Molecular polar surface area (PSA)

Molecular polar surface area (PSA) [20] is a descriptor that has been shown to correlate well with passive molecular transport through membranes and therefore allows the prediction of transport properties of the drugs. Log P is estimated according to the method of Ghose, Pritchett and Crippen [21]. A number of important graphical quantities resulted from quantum chemical calculations were displayed, manipulated and interrogated. Another indicator of electrophilic addition local map is provided by the ionization potential, an overlapping of the energy of electron removal (ionization) on the electron density. In addition, the *electrostatic potential map*, an overlay of the electrostatic potential (the attraction or repulsion of a positive charge for a molecule) on the electron density, is valuable for describing the overall distribution of molecular charge, as well as to predict the sites of electrophilic addition. Another indicator of the electrophilic addition is supplied by the *local ionization potential map*, an overlapping of the energy of electron removal (ionization) on the electron density. In the end, an indicator of nucleophilic addition is offered by the $|LUMO|$ *map*, an overlap of the absolute value of the lowest unoccupied molecular orbital (LUMO).

2.1.2. Frontier molecular orbital analysis

The molecular orbital analysis of the Frontier molecular orbitals (FMOs) plays an essential role in the chemical stability of a molecule and in the interactions between atoms. They provide information that can be used to predict the characteristics of molecules such as optical properties and biological activities. Between them, the most important are the highest occupied molecular orbital (HOMO) and the lowest unoccupied molecular orbital (LUMO). The

Compounds	R_6	R_7	R_8
NF:1-Ethyl-6-fluoro-7-(piperazin-1-yl)-1,4-dihydro-4-oxo-quinoline-3-carboxylic acid	F	Piperazinyl	H
FPQ50:1-Ethyl-6-fluoro-7-(piperazin-1-yl)-8-chloro-1,4-dihydro-4-oxo-quinoline-3-carboxylic acid [20]	F	Piperazinyl	Cl
PF:1-Ethyl-6-fluoro-7-(4-methyl-piperazin-1-yl)-1,4-dihydro-4-oxo-quinoline-3-carboxylic acid	F	4-Methyl-piperazinyl	H
FPQ51:1-Ethyl-6-fluoro-7-(4-methyl-piperazin-1-yl)-8-chloro-1,4-dihydro −4-oxo-quinoline-3-carboxylic acid	F	4-Methyl-piperazinyl	Cl
FPQ27:1-Ethyl-6-fluoro-7-(3-methyl-piperazin-1-yl)-1,4-dihydro-4-oxo-quinoline-3-carboxylic acid	F	3-Methyl-piperazinyl	H
FPQ29.HCl:1-Ethyl-6-fluoro-7-(3-methyl-piperazin-1-yl)-8-chloro-1,4-dihydro-4-oxo-quinoline-3-carboxylic acid . hydrochloride	F	3-Methyl-piperazinyl	Cl
FPQ35:1-Ethyl-6-fluoro-7-(pyrrolidin-1-yl)-1,4-dihydro-4-oxo-quinoline −3-carboxylic acid	F	Pyrrolidinyl	H
FPQ36:1-Ethyl-6-fluoro-7-(pyrrolidin-1-yl)-8-chloro-1,4-dihydro-4-oxo-quinoline-3-carboxylic acid	F	Pyrrolidinyl	Cl
FPQ32:1-Ethyl-6-fluoro-7-(piperidin-1-yl)-1,4-dihydro-4-oxo-quinoline-3-carboxylic acid	F	Piperidinyl	H
FPQ33:1-Ethyl-6-fluoro-7-(piperidin-1-yl)-8-chloro-1,4-dihydro-4-oxo-quinoline-3-carboxylic acid	F	Piperidinyl	Cl
Q83:1-Ethyl-6-fluoro-7-(4-methyl-piperidin-1-yl)-1,4-dihydro-4-oxo-quinoline-3-carboxylic acid	F	4-Methyl-piperidinyl	H
Q85:1-Ethyl-6-fluoro-7-(4-methyl-piperidin-1-yl)-8-chloro-1,4-dihydro-4-oxo-quinoline-3-carboxylic acid	F	4-Methyl-piperidinyl	Cl
FPQ24:1-Ethyl-6-fluoro-7-(3-methyl-piperidin-1-yl)-1,4-dihydro-4-oxo-quinoline-3-carboxylic acid	F	3-Methyl-piperidinyl	H
FPQ30:1-Ethyl-6-fluoro-7-(3-methyl-piperidin-1-yl)-8-chloro-1,4-dihydro-4-oxo-quinoline-3-carboxylic acid	F	3-Methyl-piperidinyl	Cl
FPQ25:1-Ethyl-6-fluoro-7-(morpholin-1-yl)-1,4-dihydro-4-oxo-quinoline-3-carboxylic acid	F	Morfolinyl	H
FPQ28:1-Ethyl-6-fluoro-7-(morpholin-1-yl)-8-chloro-1,4-dihydro-4-oxo-quinoline-3-carboxylic acid	F	Morfolinyl	Cl
NClX:1-Ethyl-6-chloro-7-(piperazin-1-yl)-1,4-dihydro-4-oxo-quinoline-3-carboxylic acid	Cl	Piperazinyl	H
6ClPQ50:1-Ethyl-6,8-dichloro-7-(piperazin-1-yl)-1,4-dihydro-4-oxo-quinoline-3-carboxylic acid	Cl	Piperazinyl	Cl
PClX:1-Ethyl-6-chloro-7-(4-methyl-piperazin-1-yl)-1,4-dihydro-4-oxo-quinoline-3-carboxylic acid	Cl	4-Methyl-piperazinyl	H
6ClPQ51:1-Ethyl-6,8-dichloro-7-(4-methyl-piperazin-1-yl)-1,4-dihydro −4-oxo-quinoline-3-carboxylic acid	Cl	4-Methyl-piperazinyl	Cl
6ClPQ27:1-Ethyl-6-chloro7-(3-methyl-piperazin-1-yl)-1,4-dihydro-4-oxo-quinoline-3-carboxylic acid	Cl	3-Methyl-piperazinyl	H

Compounds	R_6	R_7	R_8
6ClPQ29:1-Ethyl-6,8-dichloro-7-(3-methyl-piperazin-1-yl)-1,4-dihydro-4-oxo-quinoline-3-carboxylic acid	Cl	3-Methyl-piperazinyl	Cl
6ClPQ35:1-Ethyl-6-chloro-7-(pyrrolidin-1-yl)-1,4-dihydro-4-oxo-quinoline-3-carboxylic acid	Cl	Pyrrolidinyl	H
6ClPQ36:1-Ethyl-6,8-dichloro-7-(pyrrolidin-1-yl)-1,4-dihydro-4-oxo-quinoline-3-carboxylic acid	Cl	Pyrrolidinyl	Cl
6ClPQ32:1-Ethyl-6-chloro-7-(piperidin-1-yl)-1,4-dihydro-4-oxo-quinoline-3-carboxylic acid	Cl	Piperidinyl	H
6ClPQ33:1-Ethyl-6,8-dichloro-7-(piperidin-1-yl)-1,4-dihydro-4-oxo-quinoline-3-carboxylic acid	Cl	Piperidinyl	Cl
Q80:1-Ethyl-6-chloro-7-(4-methyl-piperidin-1-yl)-1,4-dihydro-4-oxo-quinoline-3-carboxylic acid	Cl	4-Methyl-piperidinyl	H
Q87:1-Ethyl-6,8-dichloro-7-(4-methyl-piperidin-1-yl)-1,4-dihydro-4-oxo-quinoline-3-carboxylic acid	Cl	4-Methyl-piperidinyl	Cl
6ClPQ24:1-Ethyl-6-chloro-7-(3-methyl-piperidin-1-yl)-1,4-dihydro-4-oxo-quinoline-3-carboxylic acid	Cl	3-Methyl-piperidinyl	H
6ClPQ30:1-Ethyl-6,8-dichloro-7-(3-methyl-piperidin-1-yl)-1,4-dihydro-4-oxo-quinoline-3-carboxylic acid	Cl	3-Methyl-piperidinyl	Cl
6ClPQ25:1-Ethyl-6-chloro-7-(morpholin-1-yl)-1,4-dihydro-4-oxo-quinoline-3-carboxylic acid	Cl	Morfolinyl	H
6ClPQ28:1-Ethyl-6,8-dichloro-7-(morpholin-1-yl)-1,4-dihydro-4-oxo-quinoline-3-carboxylic acid	Cl	Morfolinyl	Cl

Table 1. The structure of the quinolone compounds.

HOMO represents the ability of a molecule to donate an electron, while the LUMO represents the ability to accept an electron [22, 23]. The HOMO and LUMO, calculated at the B3LYP/6-31G* level, can be seen in **Figure 3** for the gas phase, for the quinolones FPQ 28 and 6ClPQ 28 (compounds that showed good activity against MRSA [19]). The graphic has 'blue and red' regions. These correspond to positive and negative values of the orbital.

For the HOMO of 7-piperazinyl-8-unsubstituted-quinolones, electron density of NF, PF and FPQ27 is localized on piperazine heterocyclic, on aromatic ring and on 4-oxo group. For the HOMO of 7-piperazinyl-8-chloro-quinolones, electron density of FPQ 50 and FPQ 51 is localized on piperazine heterocyclic; for FPQ29 compound, electron density is localized on piperazine heterocyclic and C6, C8 and C10 atoms from aromatic ring. For the HOMO of 7-piperidinyl-8-unsubstituted-quinolones, electron density of Q 83, FPQ 24 and FPQ 32is localized on piperidine heterocyclic, and on C6, C7 and C8 atoms from aromatic ring. For the HOMO of 7-piperidinyl-8-chloro-quinolones, electron density of Q 85, FPQ 30 and FPQ 33is localized on piperidine heterocyclic, on C6, C7 and C8 atoms from aromatic ring and on chlorine atom. For the HOMO of 7-morpholinyl-8-unsubstituted-quinolone, FPQ 25 electron density is localized on morpholine heterocyclic, on aromatic ring and on 4-oxo group. For the HOMO of 7-morpholinyl-8-chloro-quinolone, FPQ 28 electron density is localized on

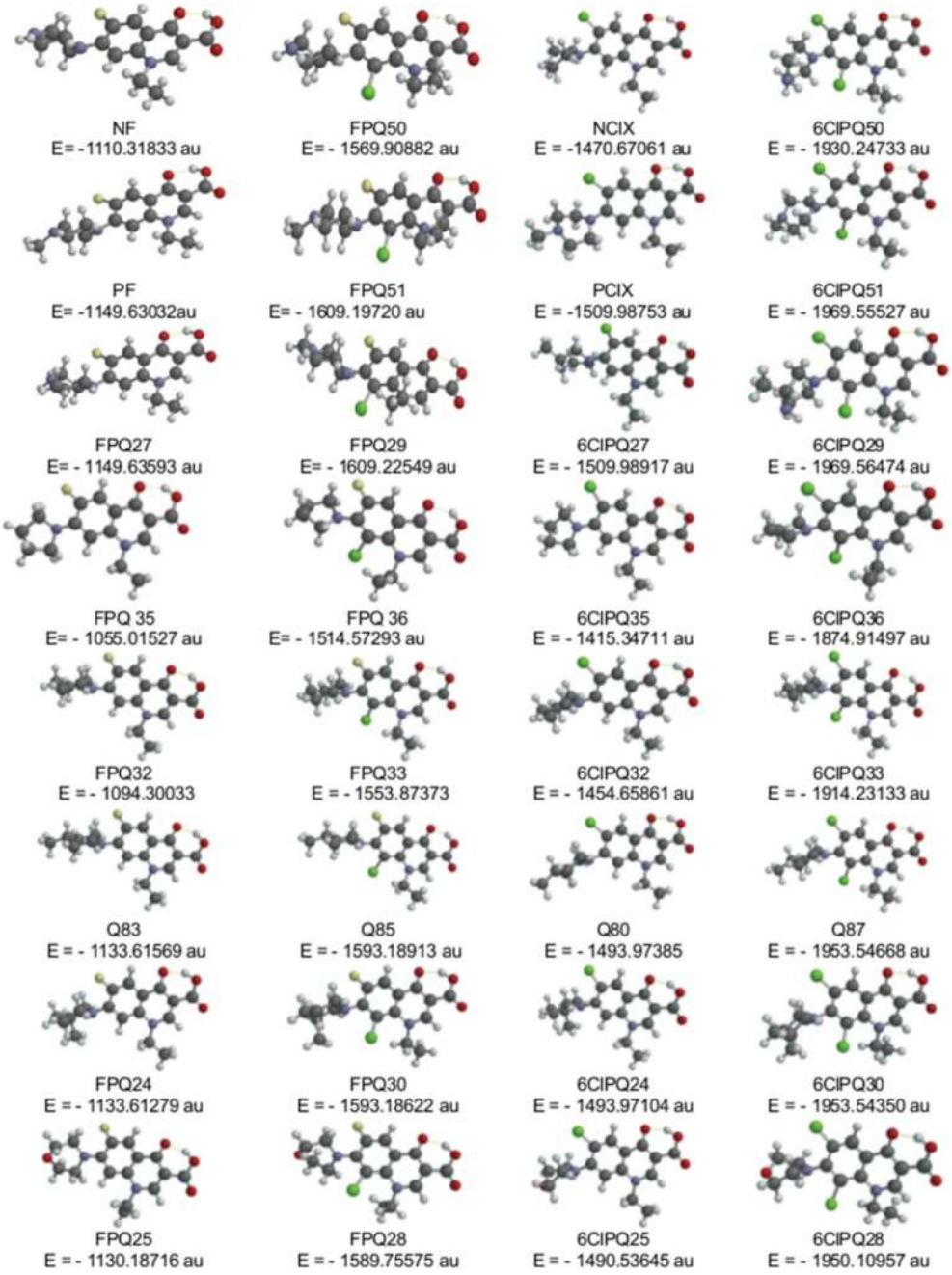

Figure 2. Optimized geometry of quinolone compounds.

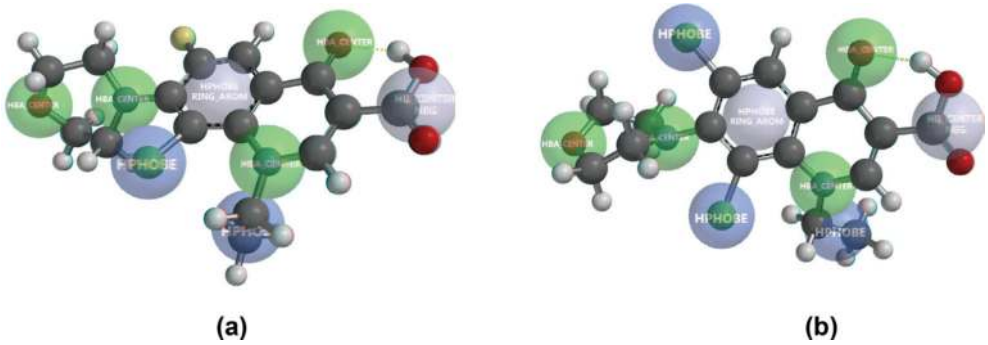

Figure 3. HBA/HBD and ±Centers, Hydrophobe centers of 8-chloro-quinolone compounds: (a) FQ28 (b) 6ClPQ28.

morpholine heterocyclic, on aromatic ring, on 4-oxo group and on chlorine atom. For the HOMO of 7-pyrrolidinyl-8-unsubstituted-quinolone, FPQ 35 electron density is localized on pyrrolidine heterocyclic, on aromatic ring and on 4-oxo group. For the HOMO of 7-pyrrolidinyl-8-chloro-quinolone, FPQ 36 electron density is localized on pyrrolidine heterocyclic, on aromatic ring, on 4-oxo group and on chlorine atom. For the LUMO of 7-substituted-8-unsubstituted-quinolones, NF, PF, FPQ27, O 83, FPQ 24, FPQ 32, electron density of FPQ 25 and FPQ 35 is localized on 4-piridinona ring and on aromatic ring. For the LUMO of 7-substituted-8-chloro-quinolones, electron density of FPQ 50, FPQ 51, FPQ29, O 85, FPQ 30, FPQ 33, FPQ 28 and FPQ 36 is localized on 4-piridinona ring, on aromatic ring B and on chlorine atom. For the 6-cloroqinolones, the electron density is located in the same manner as the corresponding fluoroquinolones.

The *frontier orbital gap* helps to characterize chemical reactivity of the molecule (**Table 2**). HOMO and LUMOs determine the way in which it interacts with other species. The introduction of the electron-withdrawing substituent (chlorine) at position C 8 in quinolone compounds decreases the HOMO-LUMO gap as compared to their corresponding 8-unsubstituted quinolone compounds (**Figure 4**).

2.1.3. Molecular electrostatic potential (MEP)

Molecular electrostatic potential (MEP) has been evaluated using B3LYP method with the basis set 6-31G* to investigate the chemical reactivity of a molecule. The MEP is especially important for the identification of the reactive sites of nucleophilic or electrophilic attack in hydrogen-bonding interactions and for the understanding of the process of biological recognition [21, 22]. An electrostatic potential map for quinolone compounds shows hydrophilic regions in red (negative potential) and blue (positive potential) and hydrophobic regions in green. In **Figure 5** can be viewed the MEP of the quinolones FPQ28 and 6ClPQ28.

The **local ionization potential map** provides another indicator of electrophilic addition; the local ionization map is an overlay of the energy of electron removal (ionization) on the

Compounds	Molecular properties									
	Dipole moment (debye)	E HOMO (eV)	E LUMO (eV)	HOMO-LUMO GAP	Polarizability (10^{-30} m^3)	PSA(Å^2)	Ovality	Log P	HBA count	HBD count
NF	12.76	−5.76	−1.41	4.35	65.09	56.587	1.45	1.37	5	1
FPQ50	8.71	−6.00	−2.02	3.98	66.33	57.344	1.46	1.92	5	1
PF	12.36	−5.77	−1.43	4.34	66.65	46.369	1.48	1.74	5	1
FPQ51	8.91	−5.79	−1.97	3.82	67.92	46.808	1.49	2.30	5	1
FPQ27	12.86	−5.76	−1.40	4.36	66.57	56.053	1.48	1.68	5	1
FPQ29	9.10	−6.01	−1.96	4.05	67.80	56.717	1.49	2.24	5	1
FPQ35	12.50	−5.77	−1.39	4.38	64.18	44.034	1.43	2.30	4	1
FPQ36	8.83	−6.14	−1.97	4.17	65.44	44.405	1.45	2.86	4	1
FPQ32	9.49	−6.63	−1.82	−4.81	65.58	45.402	1.46	2.72	4	1
FPQ33	8.28	−6.33	−2.05	4.28	66.75	44.781	1.47	3.28	4	1
Q83	9.49	−6.36	−1.82	4.54	67.06	45.389	1.49	3.05	4	1
Q85	8.29	−6.33	−2.05	4.58	68.23	44.785	1.50	3.61	4	1
FPQ24	9.48	−6.34	−1.82	4.52	67.07	45.295	1.48	3.12	4	1
FPQ30	8.23	−6.33	−2.06	4.27	68.24	44.768	1.50	3.68	4	1
FPQ25	10.15	−6.02	−1.58	4.44	64.87	51.758	1.44	1.59	5	1
FPQ28	8.26	−6.24	−1.97	4.97	66.00	51.859	1.45	2.15	5	1
NClX	8.80	−6.08	−1.93	4.15	65.98	57.537	1.47	1.77	5	1
6ClPQ50	7.81	−6.06	−2.11	3.95	67.11	56.756	1.48	2.32	5	1
PClX	11.84	−5.84	−1.59	4.25	67.42	46.688	1.49	2.14	5	1
6ClPQ51	8.69	−5.77	−2.07	3.07	68.72	46.277	1.51	2.70	5	1
6ClPQ27	8.56	−6.13	−1.93	4.20	67.46	57.339	1.59	2.08	5	1
6ClPQ29	8.00	−6.04	−2.10	3.94	68.60	56.469	1.51	2.64	5	1
6ClPQ35	12.16	−5.92	−1.54	4.38	64.92	44.303	1.44	2.70	4	1
6ClPQ36	8.51	−6.05	−2.09	3.96	66.27	43.934	1.47	3.26	4	1
6ClPQ32	9.48	−6.25	−1.89	4.36	66.39	44.937	1.47	3.12	4	1
6ClPQ33	8.26	−6.19	−2.11	4.08	67.57	44.194	1.49	3.68	4	1
Q80	9.47	−6.26	−1.89	5.07	67.86	44.979	1.50	3.45	4	1
Q87	8.26	−6.19	−2.12	4.07	69.04	44.205	1.51	4.01	4	1
6ClPQ24	9.47	−6.24	−1.89	4.35	67.88	44.863	1.50	3.52	4	1
6ClPQ30	8.27	−6.19	−2.12	4.07	69.05	44.304	1.51	4.08	4	1
6ClPQ25	7.85	−6.26	−1.97	4.29	65.69	52.427	1.46	1.99	5	1
6ClPQ28	6.68	−6.20	−2.20	−4.00	66.86	51.596	1.48	2.55	5	1

Table 2. Molecular properties for CPK model computations for quinolone compounds using Spartan'14 V1.1.4 software.

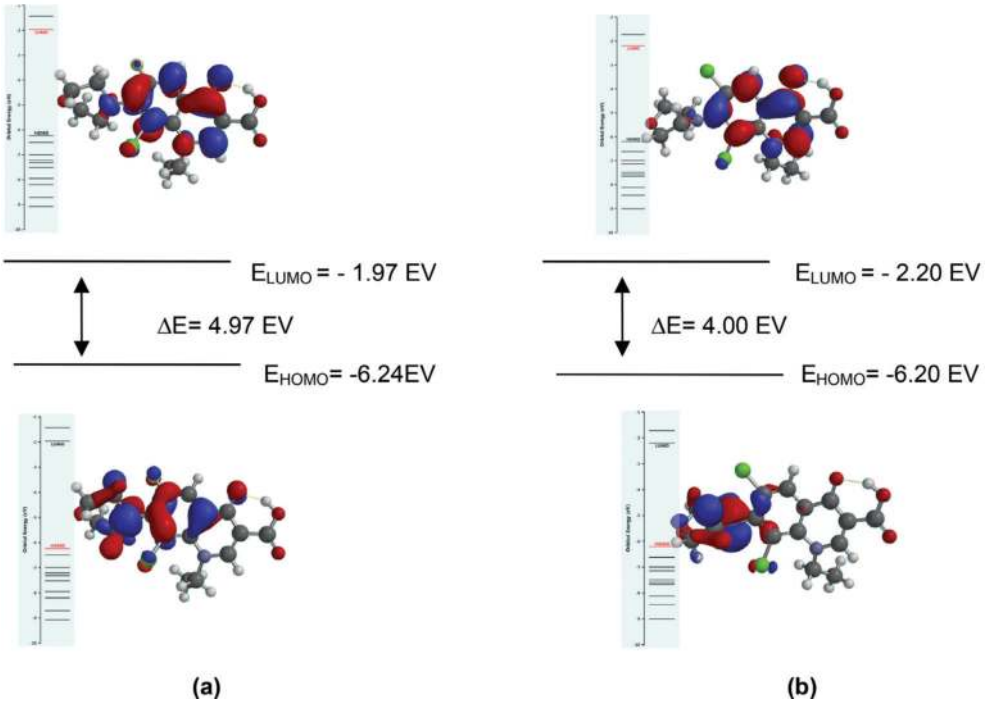

Figure 4. HOMO, LUMO surfaces of 8-chloro-quinolone compounds: (a) FQ28 (b) 6ClPQ28.

electron density (**Figure 6**). **|LUMO| map**, map that represents a superposition of the absolute value of the lowest unoccupied molecular orbital (the LUMO) on the electron density, provides another indicator of the nucleophilic addition (**Figure 7**).

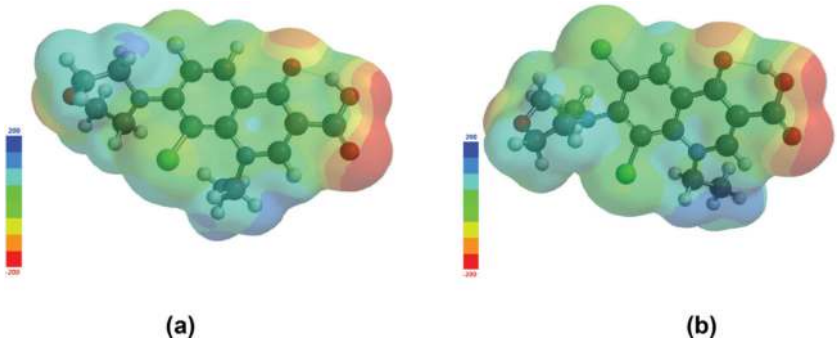

Figure 5. The optimized geometry and electrostatic potential pattern of the surface of (a) FPQ 28 and (b) 6ClPQ 28 (red—negative, high electron density, blue—positive area, low electron density).

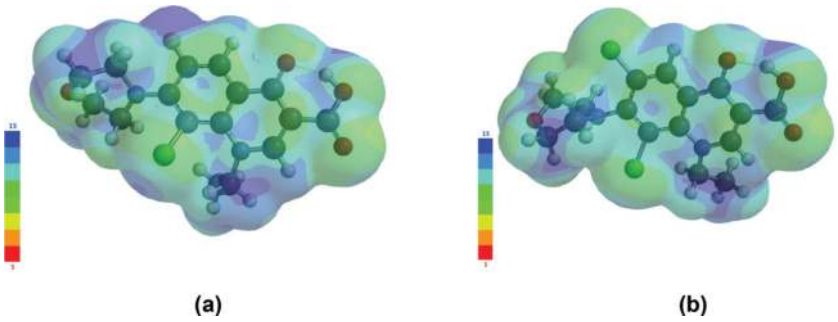

Figure 6. The optimized geometry and local ionization potential map of (a) FPQ 28 and (b) 6ClPQ 28.

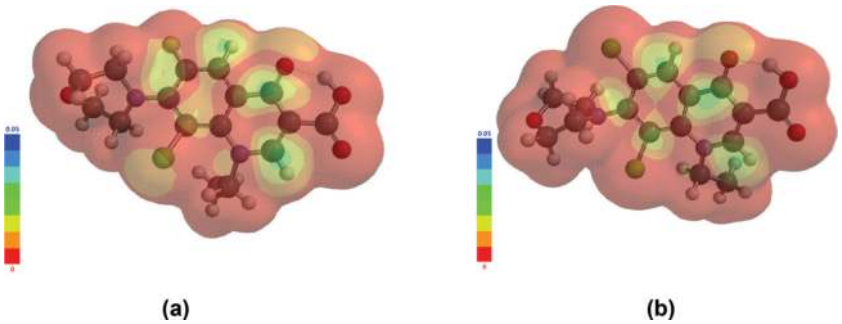

Figure 7. The optimized geometry and ILUMOI map of (a) FPQ 28 and (b) 6ClPQ 28.

2.2. Molecular docking

The steps to go through to explore protein-ligand interaction using docking are as follows: set up the binding site in a Molecule Project, import the dock ligands to a Molecule Table and inspect the docking results. The docking studies have been carried out using CLC Drug Discovery Workbench Software. The score and hydrogen bonds formed with the amino acids from group interaction atoms are used to predict the binding modes, the binding affinities and the orientation of the docked quinolone compounds (**Figure 8a–c**, **e**, **f**, **h**) in the active site of the protein receptor (**Table 3**). The docking score used in the Drug Discovery Workbench is the $PLANTS_{PLP}$ score [24]. The protein-ligand complex has been realized based on the X-ray structure of *S. aureus* DNA GYRASE, who was downloaded from the Protein Data Bank (PDB ID: 2XCT) [17].

2.2.1. Docking method validation

It ensures that the ligand orientations and position obtained from the molecular docking studies are valid and reasonable potential binding modes of ligands; the docking methods and parameters used have been validated by redocking (**Figure 8d**, **f**).

http://dx.doi.org/10.5772/intechopen.72995

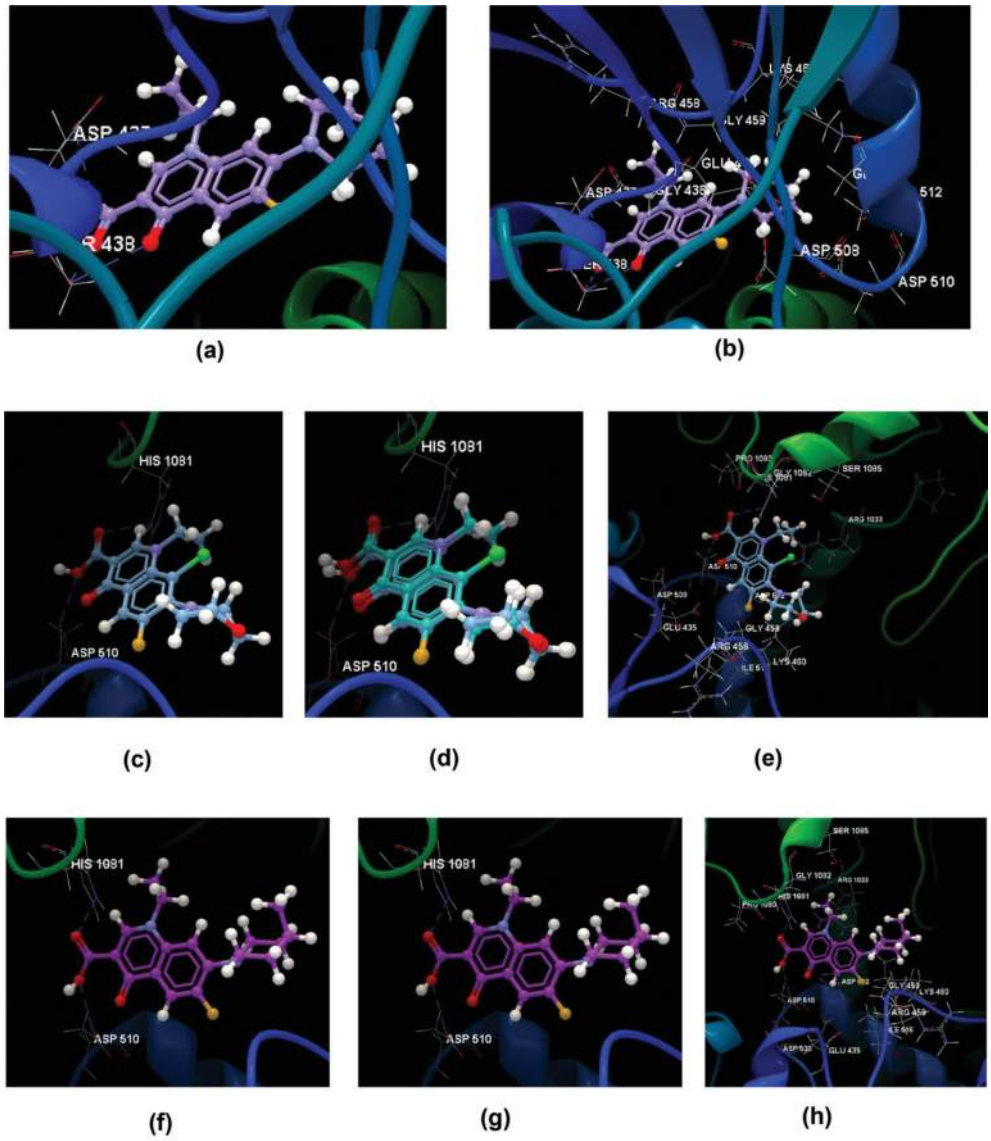

Figure 8. Molecular docking studies with 2XCT receptor. (a) Docking pose of the co-crystallized ligand CP. (b) Docking pose of the co-crystallized ligand CP interacting with residues in the binding site. (c) Docking pose of FPQ 28. (d) Docking validation of FPQ 28. (e) Docking pose of the FPQ 28 interacting with residues in the binding site. (f) Docking pose of Q 83. (g) Docking validation of Q 83. (h) Docking pose of the Q 83 interacting with residues in the binding site.

2.2.2. Determining molecular properties

Using the "Calculate Molecular Properties" tool it have been calculated important molecular properties such as logP, number of hydrogen bond donors, number of hydrogen bond acceptors

Ligand	Score/ RMSD (Å)	Group interaction/hydrogen bond	Bond length (Å)
CP	−37.27/ 0.79	*ASP510, ASP508, ASP512, GLY513, LYS460, GLY459,ARG458, GLU435, GLY436, ASP437, SER438*	
		–O sp^2 from CO–O sp^3 from SER 438	3.065
		–O sp^2 from COOH(CO)–O sp^2 from SER 438	2.816
		–O sp^3 from COOH(OH)–O sp^2 from ASP 437	2.872
ClCP	−36.63/ 0.10	*GLU477, ASP512, ASP437, ARG458,LYS460, ASN475, GLY459, ASN476, ILE461*	
		–O sp^3 from COOH(OH)–O sp^2 from GLU 477	2.933
		–O sp^2 from COOH(CO)–N sp^2 from ARG 458	3.125
NClX	−34.82/ 0.06	*ASP512, ILE 516, LYS459, ILE461, ARG458, GLU477*	
		–O sp^2 from COOH(CO)–Nsp^3 from LYS 460	3.036
NF	−39.79/ 0.11	*LYS460, GLY459, ARG458, ILE516, GLU435, ASP512, ASP510, ASP508, ARG1033, SER1085, GLY1082, HIS1081, PRO1080*	
		–O sp^2 from COOH(CO)–N sp^2 from HIS 1081	2.765
		–O sp^3 from COOH(OH)–O sp^2 from ASP 510	2.802
6ClPQ50	−33.63/ 0.07	*ASP437, ARG458, GLY459, LYS460, ILE477, LEU462*	
		–N $sp^3$from piperazine–O sp^2 from ASP 437	2.840
		–O sp^3 from COOH(OH)–O sp^2 from LYS 460	3.149
		–O sp^3 from COOH(OH)–O sp^2 from ILE 461	3.818
FPQ 50	−38.33/ 0.19	*GLY582, GLY584, LEU583, ASP508, ASP510 ASP512,LYS460, ILE516, GLY459, ARG458, LEU457, ASP437, GLY36, GLU435, SER438, ALA439*	
		–N sp^3 from piperazine–N sp^3 from LYS 460	3.195
		–O sp^3 from COOH(OH)–O sp^2 from ASP 508	3.036
		–O sp^2 from COOH(CO)–N sp^2 from ALA 439	3.027
PClX	−36.00/ 0.04	*ASP437, ARG458, GLU477,ILE461, LYS460, GLY459,TYR1025*	
		–O sp^2 from COOH(CO)–Nsp^3 from LYS 460	2.809
		–O sp^2 from CO–Nsp^3 from LYS 460	2.919
PF	−39.89/ 0.65	*ASP512, LYS460, ILE461,GLU477 GLY459, ARG458, ARG1033*	
		–O sp^2 from CO–N sp^3 from LYS 460	2.732
		–O sp^2 from COOH(CO)–N sp^3 from LYS 460	2.934
		–O sp^3 from COOH(OH)–O sp^2 from ASP 512	2.948
6ClPQ51	−34.98/ 0.10	*ASP437, ASP512,GLY459, ARG458,GLU477, ASN476,ASN475, ILE461, LYS460*	
		–O sp^3 from COOH(OH)–O sp^2 from GLU 477	2.821
		–O sp^2 from COOH(CO)–N sp^2 from ARG 458	2.929
FPQ 51	−36.50/ 0.44	*TYR1025, ASP512, HIS515, LYS460, ILE461, LEU519, LEU462, ASN463, LYS466, VAL464, ALA467, ARG471*	
		–O sp^3 from COOH(OH)–N sp^3 from LYS 460	2.888
		–O sp^2 from COOH(CO)–N sp^3 from LYS 460	2.722

Ligand	Score/ RMSD (Å)	Group interaction/hydrogen bond	Bond length (Å)
6ClPQ27	−35.72/ 0.02	*SER438, ASP437, GLY436, GLU435, SP508, LEU457, ASP510, ILE516, ASP512, LYS460, GLY459, ARG458*	
		–O sp^3 from COOH(OH)–O sp^2 from ASP 437	2.854
		–O sp^2 from COOH(CO)–O sp^3 from SER 438	2.746
		–O sp^2 from CO–O sp^3 from SER 438	3.073
FPQ 27	−37.06/ 1.50	*ASP508, GLU435, ASP510, ASP512, ILE516, LYS460,ARG458, ARG1033, GLY459, PRO1080, HIS1081, GLY1082, SER1085*	
		–O sp^3 from COOH(OH)–O sp^2 from ASP510	3.081
		–O sp^2 from COOH(CO)–N sp^2 from HIS 1081	2.726
6ClPQ29	−32.01/ 0.16	*ASP437, ARG58, GLU477, LYS460, GLY459*	
		–O sp^3 from COOH(OH)–O sp^2 from ASP 437	2.714
		–O sp^3 from COOH(OH)–O sp^2 from ASP 437	3.389
FPQ 29	−39.67/ 0.21	*SER185, ARG1033, GLY1082, HIS1081, PRO1080, LYS460, GLY459, ASP512, ARG458, ILE516, ASP508, GLU435,ARG458*	
		–O sp^2 from COOH(CO)–N sp^2 from HIS 1081	2.768
		–O sp^3 from COOH(OH)–O sp^2 from ASP510	2.804
6ClPQ25	−35.08/ 0.32	*GLU477, ARG458, LYS460, GLY459, GLU435, ASP512*	
		–O sp^3 from COOH(OH)–Nsp^3 from LYS 460	2.978
FPQ25	−39.55/ 0.04	*LYS460, ARG458, GLY459, ILE516, GLU435, ASP512,ASP510, PRO1080, HIS1081, GLY1082, SER1084, SER1085*	
		–O sp^2 from COOH(CO)–N sp^2 from HIS 1081	2.905
		–O sp^3 from COOH(OH)–O sp^2 from ASP 510	2.632
6ClPQ28	−35.65/ 0.22	*ILE516, LYS460, GLY513, ASP512, GLY459, ARG458, GLU435, ASP510, ASP508,GLY436, ASP437, SER438, ALA439*	
		–O sp^3 from COOH(OH)–O sp^2 from ASP 437	2.968
		–O sp^2 from COOH(CO)–O sp^3 from SER 438	2.641
		–O sp^2 from CO–O sp^3 from SER 438	2.915
FPQ28	−39.63/ 0.17	*LYS460, ARG458, GLY459, ILE516, GLU435, ASP508,ASP512, ASP510, ARG1033, PRO1080, HIS1081, GLY1082, SER1085*	
		–O sp^2 from COOH(CO)–N sp^2 from HIS 1081	2.863
		–O sp^3 from COOH(OH)–O sp^2 from ASP 510	2.671
6ClPQ35	−34.10/ 0.02	*SER438, ASP437, ALA439, GLY584, GLY436, GLU435, LEU457, ARG458, GLY459, LYS460, ASP512, ILE516*	
		–O sp^2 from COOH(CO)–O sp^3 from SER 438	3.174
		–O sp^2 from COOH(CO)–N sp^2 from SER 438	3.017
		–O sp^2 from COOH(CO)–N sp^2 from ASP 437	2.995
FPQ35	−39.13/ 0.18	*GLY582, ASP508, GLY584, LEU583, ALA439,SER438, ASP437,GLY436, GLU435, ASP510, ASP510, ASP512,LEU457, ARG458, GLY459, LYS460*	
		–O sp^3 from COOH(OH)–O sp^2 from ASP 508	2.642

Ligand	Score/ RMSD (Å)	Group interaction/hydrogen bond	Bond length (Å)
6ClPQ36	−35.59/ 0.23	*ASP437, ARG458, GLU477,ILE461, LYS460, GLY459,TYR1025*	
		–O sp^2 from COOH(CO)–Nsp^3 from LYS 460	3.070
		–O sp^2 from CO–Nsp^3 from LYS 460	3.040
FPQ36	−37.23/ 0.54	*LYS460, GLY459, ILE516, GLU435, ASP508, ASP512, ASP510, ARG1033, PRO1080, HIS1081, GLY1082, SER1085*	
		–O sp^2 from COOH(CO)–N sp^2 from HIS 1081	2.896
		–O sp^3 from COOH(OH)–O sp^2 from ASP 510	2.614
Q80	−38.37/ 0.02	*ASP437, ARG458, GLU477, ILE461, LYS460, GLY459*	
		–O sp^3 from COOH(OH)–Nsp^3 from LYS 460	2.935
Q83	−42.73/ 0.07	*PRO1080, HIS1081, GLY1082, SER1085, ARG1033, ASP510, ASP508, GLU435, ASP12, ILE516, ARG458, LYS460 GLY459*	
		–O sp^3 from COOH(OH)–Osp^2 from ASP 510	2.855
		–O sp^2 from COOH(CO)–N sp^2 from HIS 1081	2.761
Q87	−34.72/ 0.04	*ASP512, ASP510, GLY513, ASP508, ILE516, LYS460, GLY459, ARG458, LEU457,GLY436, GLU435, ASP437, SER438,ALA439*	
		–O sp^3 from COOH(OH)–Osp^2 from ASP 437	2.645
		–O sp^2 from COOH(CO)–Osp^3 from SER 438	2.778
		–O sp^2 from CO–Osp^3 from SER 438	2.792
		–O sp^2 from CO–Nsp^2 from SER 438	3.239
Q85	−42.07/ 0.08	*LYS460, GLY459, ARG458, ILE516, GLU435, ASP512, ASP510, SER1084, SER1085, GLY1082, HIS1081, PRO1080*	
		–O sp^3 from COOH(OH–N sp^2 from HIS 1081	2.981
		–O sp^3 from COOH(OH)–O sp^2 from PRO1080	2.411
6ClPQ24	−37.07/ 0.27	*ASN475, ASN476, GLU477,ARG458,SER437, ILE461, LYS460, GLY459*	
		–O sp^3 from COOH(OH)–O sp^2 from GLU 477	2.962
		–O sp^2 from COOH(CO)–N sp^2 from ARG 458	2.821
FPQ24	−40.64/ 0.18	*ASP510, ASP512, GLY582, ASP508, LEU583 GLU435, ILE516, LYS460, GLY459, ARG458, GLY436, ALA439, SER438, SP437 LEU457*	
		–O sp^3 from COOH(OH)–O sp^2 from ASP 508	2.644
6ClPQ30	−37.66/ 0.0063	*ARG458, GLY459, GLU477, LYS460, ILE461, ASN475*	
		–O sp^3 from COOH(OH)–N sp^3 from LYS 460	3.060
FPQ30	−41.90/ 0.32	*ARG458, GLY459, LYS460, ILE461,LEU462, ASN463, LEU519, LYS466, MET622, HIS515, ASP512, TYR1025*	
		–O sp^3 from CO–N sp^3 from LYS 460	3.060

Ligand	Score/ RMSD (Å)	Group interaction/hydrogen bond	Bond length (Å)
6ClPQ32	−33.86/ 0.03	*SER438, ASP437, ALA439, GLY436,GLU435, LEU457, ASP510, ASP512, LYS460, ASP508, ARG458, ILE516, GLY459*	
		–O sp^2 from COOH(CO)–O sp^3 from SER 438	2.852
		–O sp^2 from CO–O sp^3 from SER 438	2.897
FPQ32	41.85/ 0.07	*SER1085, ARG458, GLY459, LYS460,ILE516, GLU435, SP508, ASP512, ARG1033, LYS462, PRO1080, HIS1081, GLY1082*	
		–O sp^2 from COOH(CO)–N sp^2 from HIS 1081	2.775
		–O sp^3 from COOH(OH)–O sp^2 from ASP 510	2.817
6ClPQ33	−35.28/ 0.57	*LYS460, ILE461, ARG458, GLU477, ASN476*	
		–O sp^2 from COOH(CO)–N sp^3 from LYS 460	3.073
FPQ33	−42.53/ 0.11	*ARG458, LYS460, GLY459, ILE516, GLU435, ASP508,ASP512, ASP510, ARG1033, PRO1080, HIS1081, GLY1082, SER1085*	
		–O sp^2 from COOH(CO)–N sp^2 from HIS 1081	2.759
		–O sp^3 from COOH(OH)–O sp^2 from ASP 510	2.830

Table 3. The list of intermolecular interactions between the ligand molecules docked with 2XCT using CLC drug discovery workbench software.

Compounds	Atoms	Weight (Daltons)	Flexible bonds	Lipinski violations	Hydrogen donors	Hydrogen acceptors	Log P
NF	41	319.33	3	0	2	6	0.68
FPQ50	41	353.78	3	0	2	6	1.31
PF	44	333.36	3	0	1	6	1.15
FPQ51	44	367.80	3	0	1	6	1.77
FPQ27	44	333.36	3	0	2	6	1.11
FPQ29	44	367.80	3	0	2	6	1.74
FPQ35	39	304.32	3	0	1	5	3.90
FPQ36	39	338.76	3	0	1	5	4.53
FPQ32	42	318.34	3	0	1	5	4.26
FPQ33	42	352.79	3	0	1	5	4.89
Q83	45	332.37	3	0	1	5	4.70
Q85	45	366.81	3	1	1	5	5.32
FPQ24	45	332.37	3	0	1	5	4.70
FPQ30	45	366.81	3	1	1	5	5.32
FPQ25	40	320.32	3	0	1	6	3.04

Compounds	Atoms	Weight (Daltons)	Flexible bonds	Lipinski violations	Hydrogen donors	Hydrogen acceptors	Log P
FPQ28	40	354.76	3	0	1	6	3.67
NClX	41	335.79	3	0	2	6	0.66
6ClPQ50	41	370.23	3	0	2	6	1.28
PClX	44	349.81	3	0	1	6	1.12
6ClPQ51	44	384.26	3	0	1	6	1.75
6ClPQ27	44	349.81	3	0	2	6	1.09
6ClPQ29	44	384.26	3	0	2	6	1.72
6ClPQ35	39	320.77	3	0	1	5	3.88
6ClPQ36	39	355.22	3	0	1	5	4.51
6ClPQ32	42	334.80	3	0	1	5	4.24
6ClPQ33	42	369.24	3	0	1	5	4.86
Q80	45	348.82	3	0	1	5	4.67
Q87	45	383.27	3	1	1	5	5.30
6ClPQ24	45	348.82	3	0	1	5	4.67
6ClPQ30	45	383.27	3	1	1	5	5.30
6ClPQ25	40	336.77	3	0	1	6	3.02
6ClPQ28	40	371.22	3	0	1	6	3.64

Table 4. Ligands with properties.

and molecular weight, parameters that can be used to evaluate if a molecule has properties that would make it a likely orally active drug, according to the Lipinski's rule of five [25].

- Number of hydrogen bond donors less than 5 (the total number of nitrogen-hydrogen and oxygen-hydrogen bonds);
- Number of hydrogen bond acceptors less than 10 (the total number of nitrogen and oxygen atoms);
- The molecular weight less than 500 Daltons;
- Log P (octanol–water partition coefficient) less than 5. The calculation of the log P is based on the XLOGP3-AA method [26].

The number of violations of the Lipinski rules gives an indication of how *drug-likeness* for a molecule is. In general, orally active drugs have fewer than two violations.

These properties can be useful for identifying potential drug-like molecules, or for removing nondrug-like molecules from a compound library before starting a large virtual screening experiment (**Table 4**).

3. Results and discussions

Molecular docking study has been performed relating to some quinolone compounds known in medical therapeutics: ciprofloxacin, norfloxacin and pefloxacin. For a correct interpretation of the data has been used in the study the corresponding compound of ciprofloxacin, ClCp.

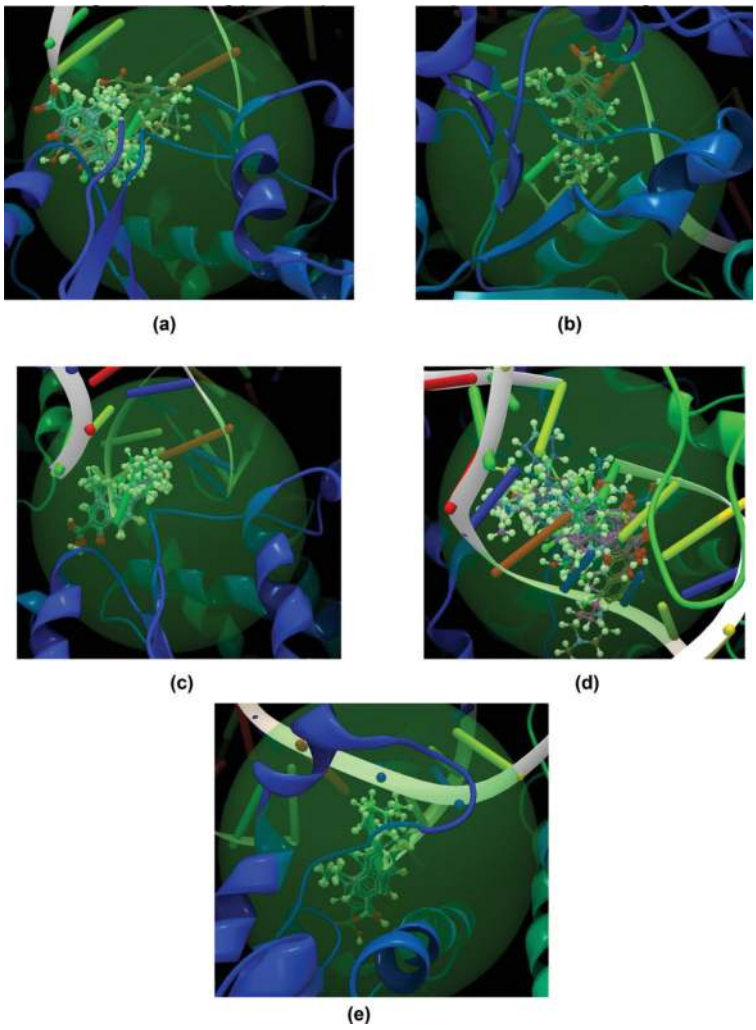

Figure 9. Docking pose of quinolone compounds in the binding site. (a) The quinolones with the similar binding mode of the co-crystallized ligand Cp. (b) The quinolones with the similar binding mode of the ClCp. (c) The quinolones with the similar binding mode of the ligand NF. (d) The quinolones with the similar binding mode of the ligand PF. (e) The quinolones with the similar binding mode of the ligand FPQ 35.

ClCp is the compound having a chlorine atom in 6-position of quinolone ring in place of fluorine atom.

The result of molecular docking study for quinolone FPQ 28, compound with a good activity '*in vitro*' against *Staphylococcus aureus* ATCC 6538 (MIC = 0.32 μg/ml) and with a good activity against MRSA [19], reveals docking score −39.63 (RMSD 0.17) and shows the occurrence of two hydrogen bonds with HIS 1081 (2.863 Å) and ASP 510 (2.671 Å) (**Figure 8c**). The orientation of the FPQ 28 is the same of NF (norfloxacin). Same orientation shows also the compounds: FPQ 32, FPQ 33, Q 83, Q 85, FPQ 27, FPQ 29, FPQ24 and FPQ 25 (**Figure 9c**). Docking score of NF compound is −39.79 (RMSD 0.11). NF shows the occurrence of two hydrogen bonds with HIS 1081 (2.863 Å) and ASP 510 (2.671 Å). The better score docking has been obtained from quinolone Q83: −42.73 (RMSD 0.07). Q83 shows the occurrence of two hydrogen bonds with HIS 1081 (2.761 Å) and ASP 510 (2.855 Å), and its orientation is the same of NF. Compound Q83 shows also a good activity '*in vitro*' against *Staphylococcus aureus* ATCC 6538 (MIC <0.125 μg/ml).

Results of the docking showed that quinolones have adopted various orientations. The same orientation with the co-crystallized ligand Cp (ciprofloxacin) shows the compound 6 ClPQ 27, 6ClPQ 28, 6ClPQ35 and Q 87. Co-crystallized Cp shows the occurrence of three hydrogen bonds with SER 438 (3.065 Å), SER 438 (2.816 Å) and ASP 437 (2.872 Å) (**Figure 9a**). The quinolones with the similar binding mode of the ClCp are 6ClPQ 51 and 6ClPQ 24 (**Figure 9b**). The quinolones with the similar binding mode of the ligand PF (pefloxacin) are 6ClPQ50, NClX, 6ClPQ 25, Q 80, FPQ 30, 6 ClPQ 33, PClX, FPQ 51, 6 ClPQ 36 and 6ClPQ 30.Docking score of PF is −39.89 (RMSD 0.65).PF shows the occurrence of three hydrogen bonds with LYS 460 (2.732 Å), LYS 460 (2.934 Å) and ASP 512 (2.948 Å) (**Figure 9d**). Same orientation shows the compounds FPQ 35, FPQ 24 and FPQ 50 (**Figure 9e**).

3.1. Drug-likeness of the quinolone compounds

According to the data presented in **Table 4**, four quinolones (Q 85, Q 87, FPQ 30 and 6ClPQ30) failed to respect one parameter (Log P > 5) of the Lipinski rules (Lipinski violation is 1). It was observed that 30 compounds of the study have zero violation of all the parameters involved in Lipinski's rule of five.

4. Conclusions

In silico molecular docking, simulation was performed to position all quinolone compounds into the preferred binding site of the protein receptor *S. aureus* DNA GYRASE, to predict the binding modes, the binding affinities and the orientation. The docking studies revealed that the all compounds showed good docking score. The docking score is a measure of the antimicrobial activity of the studied compounds. A correlation of the predicted data was observed which is obtained by molecular docking study (score docking) with the experimental data obtained from the evaluation of the antimicrobial activity against *Staphylococcus aureus* ATCC 6538 [16] of the quinolone compounds (**Figure 10a**, **b**, and **11a**, **b**).

The studies presented in this chapter show the importance of the design and the molecular docking in the discovery of new compounds with biological activity. The prediction of the

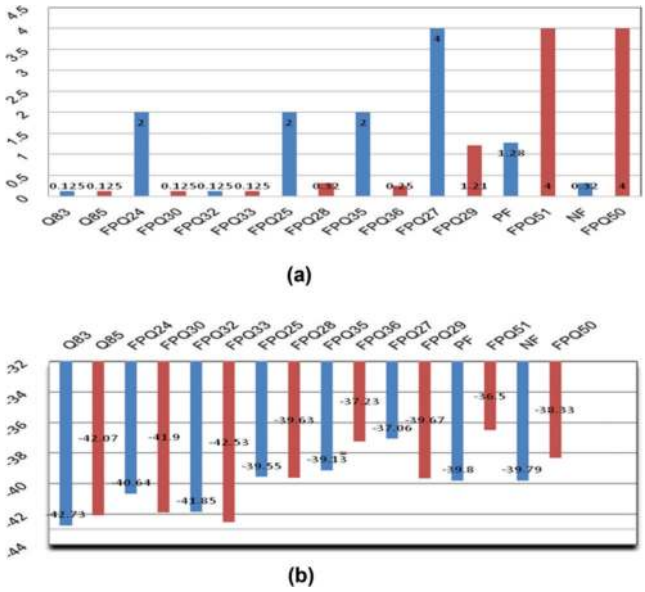

Figure 10. (a) MIC histogram of 6-fluoro-quinolone compounds. *Minimum inhibitory concentration* (MIC) of quinolone compounds against *St. aur.* ATCC 6538 (8-H-fluoroquinolones-blue, 8-Cl-fluoroquinolones-red). (b) Score docking of 6-fluoro-quinolone compounds (8-H-fluoroquinolones-blue, 8-Cl-fluoroquinolones-red).

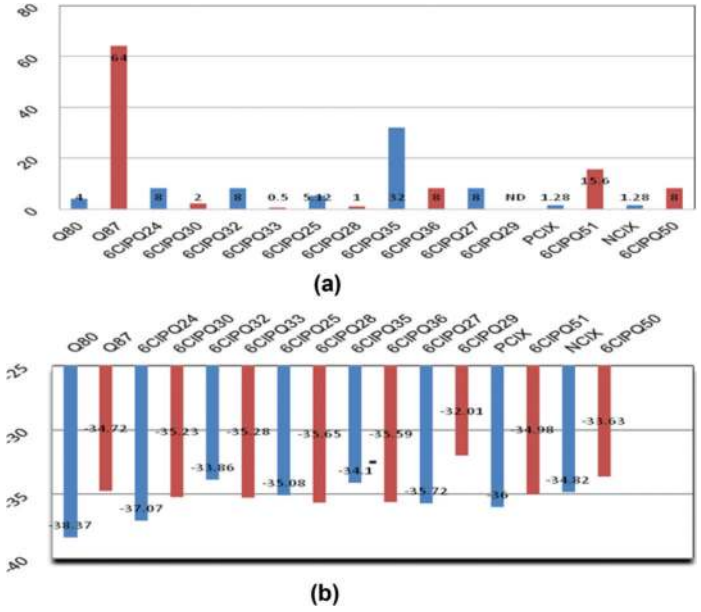

Figure 11. (a) MIC histogram of 6-chloro-quinolone compounds. Minimum inhibitory concentration (MIC) of quinolone compounds against *St. aur.* ATCC 6538 (8-H-chloroquinolones-blue, 8-Cl-chloroquinolones-red). (b). Score docking of 6-chloro-quinolone compounds (8-H-chloroquinolones-blue, 8-Cl-chloroquinolones-red).

binding affinity of a new compound (ligand) to an identified target (protein/enzyme) is a significant parameter in the development of a new drug. The prediction of the binding mode of a ligand (a new compound) to the target (protein/enzyme) by molecular simulation would allow restricting the synthesis to the most promising compounds.

Acknowledgements

This chapter has been financed through the NUCLEU Program, which is implemented with the support of ANCSI (project no. PN 09-11 01 01 and PN 09-11 01 09).

Author details

Lucia Pintilie* and Amalia Stefaniu

*Address all correspondence to: lucia.pintilie@gmail.com

National Institute of Chemical-Pharmaceutical Research and Development, Bucharest, Romania

References

[1] Meng X-Y, Zhang H-X, Mezei M, Cui M. Molecular docking: A powerful approach for structure-based drug discovery. Current Computer-Aided Drug Design. 2011;**7**:146-157. PMCID: PMC3151162 NIHMSID: NIHMS308746

[2] Ferreira FG, dos Santo RNS, Oliva G, Andricopulo AD. Molecular docking and structure-based drug design strategie. Molecules. 2015;**20**:13384-13421. DOI: 10.3390/molecules 200713384

[3] Trager E, Giblock P, Soltani S, Upadhyay AA, Rekapalli B, Peterson YK. Docking optimization, variance and promiscuity for large-scale drug-like chemical space using high performance computing architectures. Drug Discovery Today. 2016;**21**:1672-1680. DOI: 10.1016/j.drudis.2016.06.023

[4] Chen Y, Pohlaus DT, In silico docking and scoring of fragments. Drug Discovery Today Technologies. 2010;**7**:e149-e156. DOI: 10.1016/jddtec.2010.11.02

[5] Xu M, Lill MA. Induced fit docking, and the use of QM/MM methods in docking. Drug Discovery Today Technologies. 2013;**7**:e411-e418. DOI: 10.1016/jddtec.2013.02.003

[6] Alonso H, Bliznyuk AA, Gready JE. Combining docking and molecular dynamic simulations in drug design. Medicinal Research Reviews. 2006;**26**:531-568. DOI: 101002/med.20067

[7] Agarwal S, Mehrotra R. An overview of molecular docking. JSM Chemistry. 2016; **4**:1024-1027

[8] Dar AM, Mir S. Molecular docking: Approaches, types, applications and basic challenges. Journal of Analytical and Bioanalytical Techniques 2017;**8**:2. DOI: 10.4172/2155-9872.1000356

[9] Kroemer RT. Structure-based drug design: Docking and scoring. Current Protein and Peptide Science. 2007;**8**:312-328

[10] Pagadala NS, Syed K, Tuszynski J. Software for molecular docking: A review. Biophysical Reviews. 2017;**9**:1-102. DOI: 10.1007/s12551-016-0247-1

[11] Cerra B, Mostarda S, Custodi C, Macchiarulo A, Gioiello A. Integrating multicomponent flow synthesis and computational approaches for generation of a tetrahydroquinoline compound based library. Medicinal Chemical Communications. 2016;**7**:439-446. DOI: 10.1039/c5md00455a

[12] Mafud AC, Ferreira GL, Mascarenhas YP, Andricopulo AD and de Moraes J. Discovery of novel antischistomal agents by molecular modeling approaches. Trends in Parasitology. 2016;**32**:874-885. DOI: 101016/j.pt.2016.08.002

[13] Zhang X, Wang X, Liu C. Molecular docking and 3-D-QSAR study of pyranmycin derivatives against 16S rRNA a site. Journal of Molecular Structure: Theochem. 2005;**730**:85-94. DOI: 10.1016/j.theochem.2005.05.039

[14] Zhao H, Caflish A. Molecular dynamics in drug design. European Journal of Medicinal Chemistry. 2015;**91**:4-14. DOI: 10.1016/j.ejmech.2014.08.004

[15] Pintilie L. Quinolones: Synthesis and antibacterial activity. In: Bobbarala V, editor. Antimicrobial Agents. Croatia: Intech; 2012. pp. 255-272. DOI: 10.5772/33215 . Available from: https://www.intechopen.com/books/antimicrobial-agents/quinolones-synthesis-and-antibacterial-activity

[16] Pintilie L. Quinolone compounds with activity against multidrug-resistant gram-positive microorganisms. In: Bobbarala V, editor. Concepts, Compounds and the Alternatives of Antibacterials. Croatia: Intech; 2015. pp. 45-80. DOI: 10.5772/60948. Available from: https://www.intechopen.com/books/concepts-compounds-and-the-alternatives-of-antibacterials/quinolone-compounds-with-activity-against-multidrug-resistant-gram-positive-microorganisms

[17] Bax DB, Chan PF, Eggleston DS, Fosberry A, Gentry DR, Gorrec F, Giordano I, Hann M, Hennessy A, Hibbs M, Huang J, Jones E, Jones J, Brown KK, Lewis CJ, May EW, Saunders MR, Singh O, Spitzfaden CS, Shen C, Shillings A, Theobald AT, Wohlkonig A, Pearson ND, Gwynn MN. Type II A topoisomerase inhibition by a new class of antibacterial agents. Nature. 2010;**466**:935-940. DOI: 10.1038/nature09197

[18] Spartan'14 Wavefunction, Inc. Irvine, CA. Available from: www.wavefun.com

[19] Pintilie L, Dorobat O, Caproiu MT, Maganu M. Quinolone derivatives with activity against multi-drug resistant gram-positive microorganisms. Revista de Chimie. 2014;**65**: 1176-1181

[20] Martin YC. A bioavailability score. Journal of Medicinal Chemistry. 2005;**48**:3164-3170. DOI: 10.1021/jm0492002

[21] Arup K, Ghose AK, Pritchett A, Crippen GM. Atomic physicochemical parameters for three dimensional structure directed quantitative structure-activity relationships III: Modeling hydrophobic interactions. Journal of Computational Chemistry. 1988;**9**:80-90

[22] Gautam BP, Dani RK, Prasad R, Srivastava M, Yadav RA, Gondwal M. Synthesis, characterization, single crystal structural studies, antibacterial activity and dft investigations of 2-chloro-5-ethoxy-3,6-bis(methylamino)-1,4-benzoquinone. Pharmaceutica Analytica Acta. 2015;**6**. DOI: 10.4172/2153-2435.1000418

[23] Lasri J, Eitayeb NE, Ismail AI. Experimental and theoretical study of crystal and molecular structure of 1,2-di(9*H*-fluoren-9-ylidene)hydrazine. Journal of Molecular Structure. 2016;**1121**:35-45. DOI: 10.1016/j.molstruc.2016.05.044

[24] Korb O, Stützle T, Exner TE. Empirical scoring functions for advanced protein-ligand docking with PLANTS. Journal of Chemical Information and Modeling. 2009;**49**:84-96. DOI: 10.1021/ci800298z

[25] Lipinski CA, Lombardo F, Dominy BW, Feeney PJ. Experimental and computational approaches to estimate solubility and permeability in drug discovery and devel opment settings. Advanced Drug Delivery Reviews. 2001;**46**:3-26. DOI: 10.1016/S0169-409X(00)00129-0

[26] Cheng T, Zhao Y, Li X, Lin F, Xu Y, Zhang X, Li Y, Wang R. Computation of octanol-water partition coefficients by guiding an additive model with knowledge. Journal of Chemical Information and Modeling. 2007;**47**:2140-2148. DOI: 10.1021/ci700257y